Extended Abstracts of the 2009 International Conference on Solid State Devices and Materials, Sendai, 2009, pp1230-1231

Performance Evaluation of Graphene Nanoribbon Tunneling Field Effect Transistors

Kai-Tak Lam[1], S. Bala Kumar[1], Sai Kong Chin[2], Da Wei Seah[1] and Gengchiau Liang[1,2†]
[1]Deparrtment of Electrical and Computer Engineering, National University of Singapore, Singapore
[2]Institute of High Performance Computing, Singapore
[†]Phone: +65-6516-2898 E-mail: elelg@nus.edu.sg

1. Introduction

With aggressive device miniaturization, conventional complementary metal-oxide semiconductor (CMOS) transistors based on silicon are rapidly reaching their fundamental physical limits and novel device structures are required. Many studies had shown that silicon tunneling field-effect transistors (TFETs) have a smaller (<60mV/dec) subthreshold swing (*SS*), which is ideal for fast switching applications, and a lower OFF current (I_{OFF}) which can be used for low power devices. However, due to the dependency of tunneling mechanism, the ON current (I_{ON}) is too small and novel electronic materials which have high carrier mobility can be used to improve the performance of TFET [1-3]. In this regard, alternative electrical material can be used, such as graphene related materials, which have attracted a lot of attention in the device community recently since the physical realization of thermodynamically stable graphene sheets. More specifically, the one dimensional graphene nanoribbons (GNRs) which inherited the excellent electrical properties of the planar graphene sheet such as high carrier mobility [4], as well as exhibiting some of their own unique properties such as the variation of energy gap by change the ribbon width [5], can be a good material for TFET implementation. While previous computational studies on GNR TFET such as Zhang, *et al.* [6] which employed the WKB approximation were not able to properly capture the full quantum tunneling event, utilization of π-orbital tight-binding method as in Zhao *et al.* [7] requires a large amount of computational resources and inhibits the investigations of larger system. As such, a mode-space quantum simulator based on the Dirac equation is developed for the study of GNR TFET and in this work, we present our computational study on the device characteristics of GNR TFET at different ribbon width and doping concentrations.

2. Simulation model

A side view schematic of the device structure used in the simulation is shown in Fig. 1(a) which is similar to a double gate CMOS device, with the device material replaced with GNR. The width (*W*) of the GNR (shown in Fig. 1(b) is an important parameter for GNR devices and three different widths are studied in this work. A quantum simulator, which couples the Dirac equation [8] that describes the electronic interaction in GNR, with the non-equilibrium Green's function approach [9], is used to simulate the carrier transport of the GNR TFET. This novel method, which we termed Dirac tight-binding approach, is first validated by calculating the energy spectra of GNRs with different widths and comparing them to π-orbtial tight-binding calculations. The spectra are shown in Fig. 2 which exhibit matching results at low k-vectors for the widths of (a) 1.1, (b) 1.2 and (c) 1.3 nm. After the model validation, full device simulations, with the Poisson's potential solved

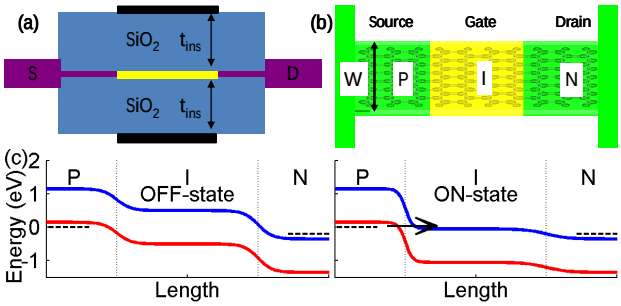

Fig. 1: (a) A side view schematic of a double-gate graphene nanoribbon tunneling field effect transistor (GNR TFET). The gate insulator is silicon dioxide with a thickness (t_{ins}) of 1nm in this work. (b) The top view of the GNR TFET. The source and drain are doped with holes and electrons respectively and different ribbon width are used. The channel length of the device is kept at a constant of 10nm. (c) A schematic of the energy band of the *p-i-n* structure during (left) OFF-state and (right) ON-state. The conduction and valance bands are represented by the blue and red lines, respectively. Ideally, OFF-state current is low due to the long tunneling width while ON-state current is high due to the short tunneling width.

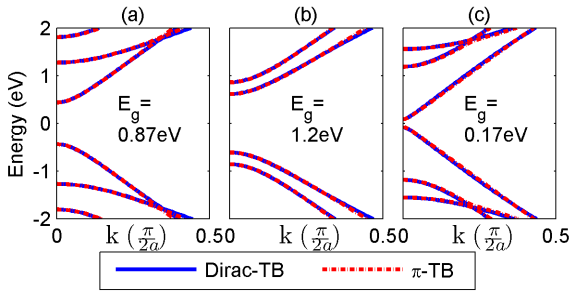

Fig. 2: The comparison of GNR energy spectra with widths of (a) 1.1, (b) 1.2 and (c) 1.3 nm between Dirac tight-binding (blue, solid) and π-orbital tight-binding (red, dash-dot) methods. The spectra from the different methods are matching at low k-vector and the variations in energy gap are also reproduced in Dirac tight-binding method.

self-consistently, for devices with different widths and a similar channel length of 10nm, are carried out at a drain bias of 0.6V to extract the I_{DS}-V_{GS} current characteristics. For the 1D GNR TFET, the contacts have a carrier doping concentration of 0.71/μm, with the source doped with holes and the drain with electrons to simulate a *p-i-n* structure.

3. Results and discussion

As shown in Fig. 3, although the width is varied slightly from 1.1nm to 1.3 nm, the performance changes dramatically. The I_{ON}/I_{OFF} ratio changes from 1.87×10^3 to 4.36×10^5 to 1.10, and *SS* changes from 74 to 43 mV/dec to infinity for 1.1, 1.2, and 1.3nm wide GNR FETs, respectively. This variation can be explained by the change in the energy band gap as the width changes as shown in Fig. 2. The bandgap of 1.2nm cases is 1.2 eV while that of 1.3nm GNRs drops to 0.17 eV. We next focus on device physics of GNR TFETs and the local current spectra (J_n) are plotted for different gate bias (V_{GS}) of 0, 0.3 and 1V and are summarized in Fig. 4. At V_{GS}=0V, there is a high tunneling

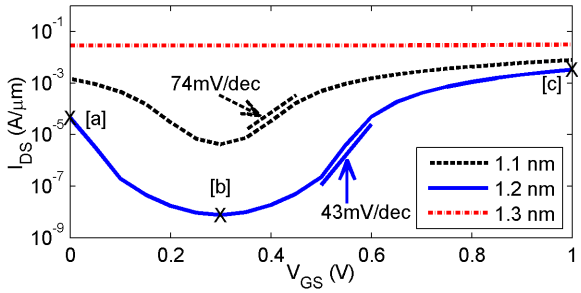

Fig. 3: The current-voltage characteristics of GNR TFET with ribbon widths of 1.1 (black, dash), 1.2 (blue, solid) and 1.3 nm (red, dash-dot). The three crosses on the blue solid line indicate the points where the local current spectra are calculated to show the device physics of GNR TFET and they corresponds to the plots in Fig. 4.

current [arrow in Fig. 4(a)] from the channel to the drain due to the proximity between the top of the valance band (E_V) of the channel and the bottom of the conduction band (E_C) at the drain. This is commonly known as band-to-band tunneling (BTBT). As V_{GS} increases, the E_C and E_V at the channel-drain interface is being pulled apart and the BTBT at the drain side decreases and at V_{GS}=0.3V, the current is mainly due to the direct tunneling between the source and the drain, indicated by the arrow in Fig. 4(b). As V_{GS} increase further, the E_C of the channel is pulled below the E_V of the source and BTBT occurs at the source-channel interface [*cf.* arrow in Fig. 4(c)]. Therefore, in 1.1nm cases, the bandgap is too small to separate these different phenomena and results in the constant high current.

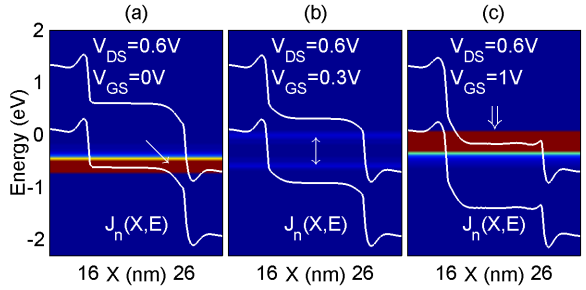

Fig. 4: The local current spectra for the GNR TFET at a gate bias (V_{GS}) of (a) 0, (b) 0.3 and (c) 1V. There is a large band-to-band tunneling (BTBT) current initially from the channel to drain, indicated by the arrow in (a) and as the V_{GS} increases, BTBT current decreases at the drain side and the OFF-state current is mainly due to direct tunneling shown by the arrow in (b). As the V_{GS} increases further the BTBT current at the source started and is the major contributor to the device current at V_{GS}=1V shown in (c).

Next, the electron doping at the drain side is lowered by an order to 0.07/μm and the I_{DS}-V_{GS} of the 1.2nm device is shown in Fig. 5(a). The lower doping device (red, dashed line) has a much smaller current at V_{GS}=0V as compared to the device with a higher drain doping (blue solid line) but have a similar current at V_{GS}=1V. By studying the J_n at the channel-drain interface at V_{GS}=0V of the higher and lower drain doping device (shown in Fig. 5(b) and (c) respectively), it is observed at for the lower drain doping device, the BTBT current can be suppressed due to the increase in tunneling width.

Lastly, the effect of different source doping concentration is simulated by changing the hole concentration at the source to 0.07/μm. The current characteristics of the 1.2nm wide lower source doping device is compared to the original control device and are shown in Fig. 6(a) as the red

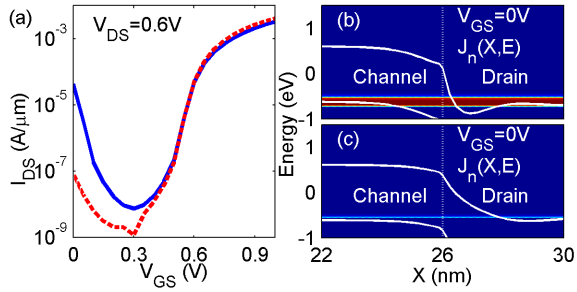

Fig. 5: (a) The current characteristics of 1.2nm with different drain doping. The blue solid line is the same device in Fig. 3 and the red dashed line is for the device with a lower drain doping of 0.07/μm. The local current spectra are plotted for the respective devices in (b) and (c) for V_{GS}=0V and it is observed that the BTBT current in the lower drain doping device is much smaller than the control device.

dashed and blue solid line respectively. In this case, the device current at VGS=1V is lowered while the current at VGS=0V is constant when compared to the control device. This is explained by the fact that there are less carrier injected into the channel from the source for the lower doping device and can be observed in the current spectrum as shown in the Fig. 6(b).

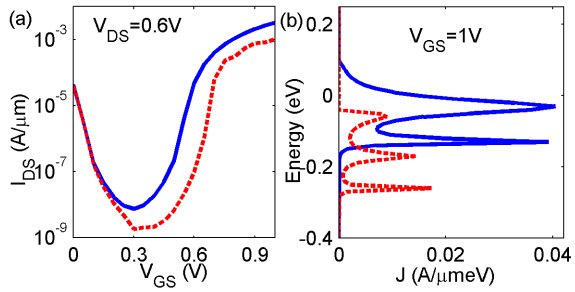

Fig. 6: (a) The current characteristics of 1.2nm with different source doping. The blue solid line is the same device in Fig. 3 and the red dashed line is for the device with a lower source doping of 0.07/μm. (b) The current spectra of the control device (blue solid) and the lower source doping device (red dashed).

4. Conclusion

The device characteristics of GNR TFET simulated with a Dirac tight-binding approach is presented in this work. The effect of ribbon width on the device performance is shown and it is found that a slight variation in width will have a vast effect on the I_{ON}/I_{OFF} ratio as well as the *SS*. The doping effects at the source and drain of GNR TFET are also investigated and it is found that the I_{ON} can be increased by increasing the doping concentration at the source and the I_{OFF} can be decreased by lowering the doping concentration at the drain. Hence the device performance of GNR TFET can be easily tuned by varying the doping concentrations at the source and drain.

Acknowledgments

This work was supported by A*STAR 082-101-0023 and MOE, Singapore under Grant Nos. R-263-000-416-112 and R-263-000-416-133.

References

[1] J. Appenzeller, *et al.*, IEEE Transactions on Electron Devices, Vol. 52, No. 12, pp. 2568 (2005). [2] E.-H. Toh, *et al.*, Appl. Phys. Lett. **91**, 243505 (2007). [3] S.O. Koswatta, *et al.*, IEEE Transactions on Electron Devices, Vol. 56, No. 3, pp. 456 (2009). [4] M.C. Lemme, IEEE Electron Device Lett., Vol. 28, No. 4, pp 282 (2007). [5] Y.-W. Son, *et al.*, Phys. Rev. Lett. **97**, 216803 (2006). [6] Q. Zhang, *et al.*, IEEE Electron Device Lett., Vol. 29, No. 12, pp 1344 (2008). [7] P. Zhao, *et al.*, Nano Lett. **9**, 684 (2009). [8] A.H. Castro Neto, *et al.*, Rev. Mod. Phys. **81**, 109 (2009). [9] S. Datta, Quantum Transport: Atom to Transistor, Cambridge University Press, New York (2005)